Topological Signatures of Globular Polymers

M. Baiesi,[1] E. Orlandini,[1,2] A. L. Stella,[1,2] and F. Zonta[1]

[1]*Dipartimento di Fisica, Università di Padova, Via Marzolo 8, I-35131 Padova, Italy*
[2]*Sezione INFN, Università di Padova, Via Marzolo 8, I-35131 Padova, Italy*

(Received 16 March 2011; published 24 June 2011)

Simulations in which a globular ring polymer with delocalized knots is separated in two interacting loops by a slipping link, or in two noninteracting globuli by a wall with a hole, show how the minimal crossing number of the knots controls the equilibrium statistics. With slipping link the ring length is divided between the loops according to a simple law, but with unexpectedly large fluctuations. These are suppressed only for unknotted loops, whose length distribution always shows a fast power-law decay. We also discover and explain a topological effect interfering with that of surface tension in the globule translocation through a membrane nanopore.

DOI: 10.1103/PhysRevLett.106.258301 PACS numbers: 82.35.Lr, 02.10.Kn, 36.20.Ey, 87.15.A−

Most often, ring polymers are experimentally studied in situations in which their topological entanglement does not change in time. However, most of our theoretical and numerical understanding of polymer statistics relies on ensemble descriptions in which the rings assume all possible topologies [1]. An open challenge is that of determining up to what extent specific permanent entanglements in the form of knots or links [2] can affect thermodynamic quantities and what is their possible role in determining peculiar behaviors when the polymer is subject to geometrical constraints interfering with the topology.

Different topologies are expected to determine different corrections to the free energy of a single ring in the limit of infinitely long chain. For example, the prime knot components of ring polymers in good solvent are weakly localized in this limit [3,4]. As a consequence, if N is the chain length, each component determines a correction $\sim k_B \ln(N)/N$ to the entropy per monomer [5,6]. Indeed, each component behaves asymptotically as a pointlike decoration which can place itself anywhere along the ring. Radically different conditions are realized below the theta temperature T_θ [7]. Indeed, in the globular phase knots are expected to delocalize. Numerical simulations indicate that the topological entanglement spreads on average on a portion of the ring whose length is proportional to N [8,9]. Fixed topology determines a finite size correction to the free energy of a globular ring, which is asymptotically negligible in comparison with that due to surface tension ($\sim N^{-1/3}$). Indeed, at a temperature $T \approx \frac{2}{3} T_\theta$, the correction per monomer has been estimated [10] as $\sim C n_c^a N^{-2}$, where $a \simeq 1.45$, n_c is the minimal number of crossings of the knot [2], and C is a remarkably large negative amplitude. Thus, n_c qualifies as a topological invariant possibly relevant for the thermodynamics of a globular ring.

In the present Letter we face the challenge of elucidating the role of this invariant, by establishing some empirical laws through which it rules the statistics of the globule when suitable local geometrical constraints are imposed. These laws, which generally hold in the presence of large fluctuations, give a precise meaning to the notion of knot delocalization. We also discover novel thermodynamic phenomena which are a peculiar consequence of topology and quantitatively explain them in terms of an ansatz for the globule free energy.

Suppose one forces a ring polymer to pass into a slipping link which divides it into two loops. The link is narrow enough to prevent the passage of topological entanglement from one loop to the other. For instance, if the ring has a composite knot with two prime trefoil (3_1) components [2], things can be arranged so that each fluctuating loop encloses one trefoil knot. The loops are kept unlinked. We model flexible ring configurations as N-step self-avoiding polygons on cubic lattice [11]. An attractive interaction J between nearest neighbor visited sites allows us to obtain a collapsed globular phase for low enough temperature T [7] (Fig. 1). A Monte Carlo simulation method adequate to preserve the ring topology is the grand-canonical

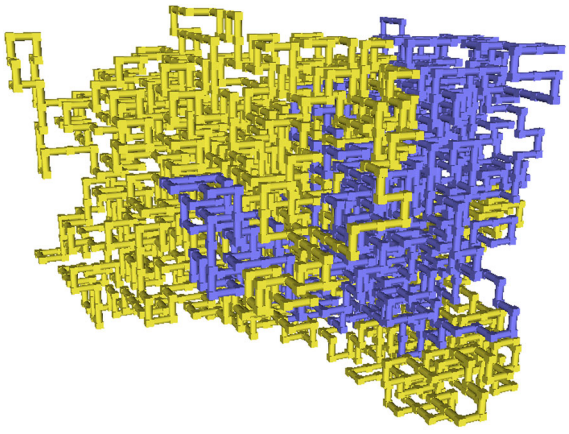

FIG. 1 (color online). $N = 2040$ globule with slip link separating a 3_1 knot in loop 1 [light gray (yellow)] from a 4_1 knot in loop 2 [dark gray (blue)].

Berg–Foester–Aragao de Carvalho–Caracciolo–Froehlich (BFACF) one [11]. However, straightforward application of BFACF to the globule meets a difficulty. Indeed, indicating by K the step fugacity and by Z_N the canonical partition function, the grand-canonical average $\langle N\rangle = \Sigma_N N K^N Z_N / \Sigma_N K^N Z_N$ does not grow continuously to $+\infty$ upon approaching from below the critical value K_c of the fugacity. To the contrary, one gets evidence of a discontinuous infinite jump right at $K = K_c$ [8]. We understand here this behavior in light of the expected [10,12] asymptotic form of Z_N:

$$\ln(Z_N) = -F(N, n_c)/kT \sim \text{const} + \mu N + \sigma N^{2/3} + (\alpha - 2)\ln(N) + \frac{C n_c^a}{N}, \quad (1)$$

where $\mu = -\ln(K_c)$, $\sigma < 0$ is the interfacial tension, and α is an unknown specific heat exponent that is expected to be independent of topology. The last term on the right-hand side of Eq. (2) is the topological correction to the total free energy F. The presence of the surface term $\sim\sigma N^{2/3}$ implies that $\langle N\rangle$ cannot diverge continuously to $+\infty$ for K approaching K_c from below. In order to allow a continuous growth of $\langle N\rangle$, we choose to multiply the usual grand-canonical weight of the ring configurations by a factor $\exp[(N - N_0)^2/\nu]$ which forces N itself to fluctuate around a value close to N_0 if ν is chosen small enough. The BFACF simulation augmented with the new statistical weight allows a quasicanonical sampling of configurations with N close to the value determined also by N_0 and ν. To improve sampling efficiency, we also implement a multiple Markov chain scheme [13] over different values of N_0 keeping K fixed. Nevertheless, the simulations need a long CPU time (months) to sample a consistent statistics. For this reason we choose to sample only at the temperature $T = 2.5J$, as in [10].

Extensive simulations of the 3_1 vs 3_1 configuration allow us to sample for various restricted ranges of N the probability density function (PDF) of l_1/N, $P(l_1/N)$, where l_1 is the fluctuating length of one of the loops [Fig. 2(a)]. Remarkably, even for large N the histogram does not seem to present the bimodal shape, indicating a dominance of configurations with large unbalance between l_1 and l_2, that was found in the good solvent case [3,8]. To the contrary, an asymptotically flat histogram seems compatible with the data. Thus, while the two loops on average share equally the total ring length [Fig. 2(b)], there are very broad fluctuations.

To gain further insight, we also simulate the case in which the loops are both unknotted. In this case strongly unbalanced situations are clearly favored. The PDF of the length of the smaller loop, say l_1, shows a power-law decay $\sim l_1^{-x}$, with $x = 1.55 \pm 0.04$ (Fig. 3). This suggests that the metric exponent of this loop is $\nu = x/d \approx 0.52$. A value of ν close to $1/2$ is consistent with the expectation of Gaussianity of a collapsed chain on relatively small length scales [14]. When, for example, only loop 2 has a 3_1 knot, while loop 1 is unknotted (∅), l_1 never grows substantially compared to N, and the same power-law behavior holds for the PDF of l_1 (Fig. 3). This law, implying $\langle l_1\rangle \sim N^{0.45(4)}$, denotes a weak localization of the unknotted loop.

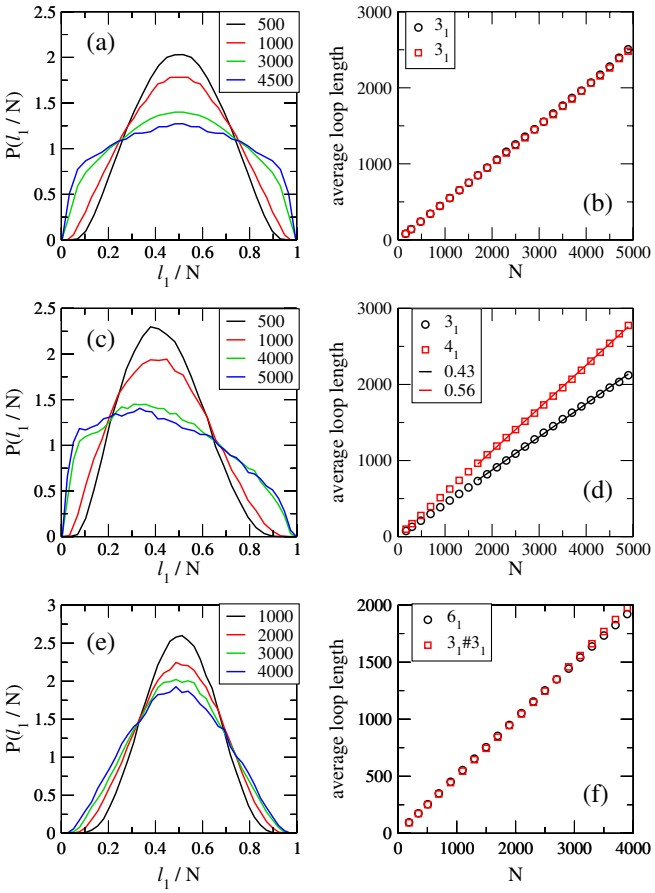

FIG. 2 (color online). (a) Histograms of $P(l_1/N)$ for 3_1 vs 3_1. Different curves correspond to different N values (see legend). (b) $\langle l_1\rangle_N$ (circles) and $\langle l_2\rangle_N$ (squares) as a function of N. (c) Histograms of $P(l_1/N)$ for 3_1 vs 4_1 and (d) corresponding average loop lengths. (e) Histograms of $P(l_1/N)$ for 6_1 (loop 1) vs $3_1\#3_1$ and (f) corresponding average loop lengths.

The above results are fully consistent with delocalization of the 3_1 knot inside the ring, since in no case a loop containing the knot displays a stable regime in which its average length is a vanishing fraction of N. Similar results hold if 3_1 is replaced by another prime knot. We further examine a competition 3_1 vs 4_1. The plots reported in Fig. 2(c) show that also in this case the lengths of the loops keep fluctuating very broadly for increasing N, while $P(l_1/N)$ is not symmetric with respect to $l_1/N = 1/2$ anymore. Quite remarkably, in this and similar competitions (3_1 vs 7_1, 4_1 vs 6_1, etc.), a simple law is well obeyed by the canonical averages $\langle l_1\rangle_N$ and $\langle l_2\rangle_N$:

$$\langle l_i\rangle_N = N\frac{n_{ci}}{n_{c1} + n_{c2}}, \qquad i = 1, 2. \quad (2)$$

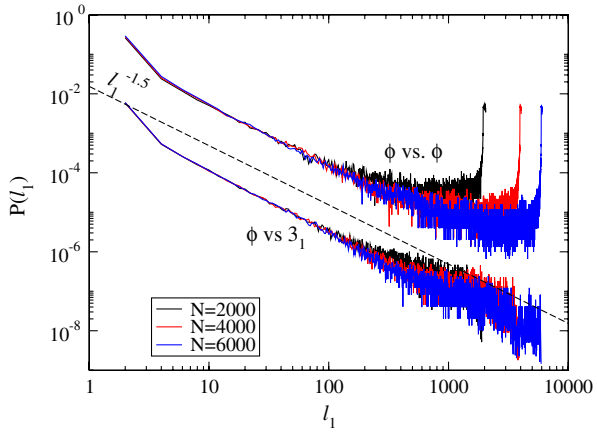

FIG. 3 (color online). Log-log plots of $P(l_1)$ for ∅ vs ∅ (upper curves, for three values of N) and ∅ vs 3_1 (lower curves, shifted one decade down). The dashed line represents a power law $l_1^{-1.5}$. Each N includes the statistics in the interval $[N-50, N+50]$: this does not alter the power-law tail and increases the statistics considerably.

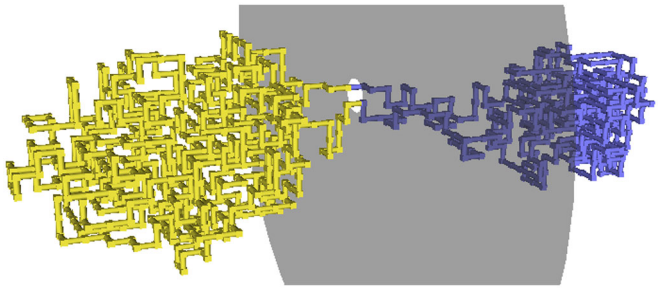

FIG. 4 (color online). Example of a wall-globule system. The hole (white) separates the $N = 1000$ chain into two globuli with 3_1 knot (colored differently).

In this case the loop with the 3_1 knot obtains on average a fraction of the chain length equal to $3/7 \approx 0.43$, while $4/7 \approx 0.56$ go to the loop with 4_1 knot. This is evidenced in Fig. 2(d) by the linear fits of the average loop lengths as a function of N. The law in Eq. (2), which we can of course test only for relatively low values of the n_{ci}'s, highlights the key role played by n_c in the delocalized regime. This role is further emphasized by considering the competition of two knots that are different but with the same n_c. Figures 2(e) and 2(f) show the results for $3_1\#3_1$ vs 6_1. We see that, while the fluctuations remain very broad, also in this case Eq. (2) is still obeyed to a reasonable approximation. In addition the shape of the histograms is almost as symmetric as in the 3_1 vs 3_1 case. However, the possible convergence towards a flat histogram is definitely slower than in that case. These results suggest that the number of prime components of a knot is not a relevant invariant, unlike in the swollen regime.

In experiments the slipping link could be, e.g., a short (unknotted) ring which is not linked to the knotted one, but just constrains it to pass through its interior. To discover further consequences of topology in the globular phase we replace the slipping link by a sufficiently narrow hole in an impenetrable wall (Fig. 4). This schematizes the translocation of a ring polymer through a membrane or solid state nanopore, a phenomenon that, thanks to recent progress in nanotechnology, can be investigated experimentally [15,16]. A related biological issue is the effect that knots may have on the ejection process of packed viral DNA into the host cell [17,18]. Because of the presence of the wall the two loops do not interact anymore and can be considered as two independent, knotted globuli in competition. As shown in Fig. 5 for a case with two different knots having however the same $n_{c1} = n_{c2} = 6$, $P(l_1/N)$ develops two remarkably symmetric peaks for $N \gtrsim 1000$, which become separated by a very high free energy barrier already at $N \approx 2300$. Similar results are obtained for the simpler case 3_1 vs 3_1.

The situation turns out to be totally different when $n_{c1} \neq n_{c2}$. In these cases we observe an asymmetry, indicating a

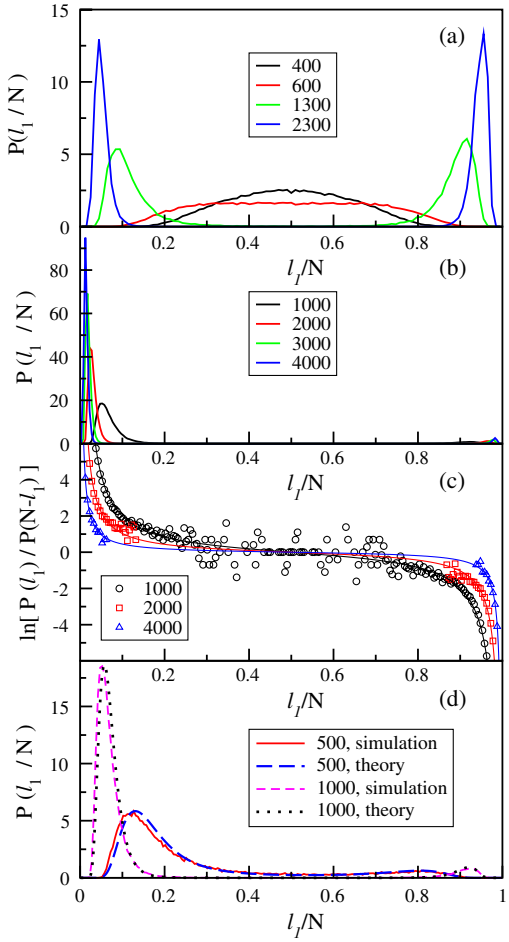

FIG. 5 (color online). (a) Histograms of $P(l_1/N)$ for $3_1\#3_1$ (loop 1) vs 6_1 and (b) for 3_1 (loop 1) vs 4_1 when the two globular loops are separated by a wall. (c) Plot of $[F(l_1, n_{c1}) + F(N - l_1, n_{c2}) - F(l_1, n_{c2}) - F(N - l_1, n_{c1})]/k_BT$ vs l_1/N for the case in (b). (d) Comparison between the numerical data and the analytical prediction for the 3_1 vs 4_1 case ($N = 500$ and 1000).

clear dominance of the globular loop hosting the knot with higher n_c. This dominance becomes more and more pronounced as N increases [see Fig. 5(b) for 3_1 vs 4_1].

How topology can produce the asymmetry manifested by the above results for the wall case can be explained as follows. The equilibrium share of the ring length between the two globuli should stably minimize the free energy. Because of independence, the total free energy is simply the sum of the free energies of the two globuli. Since each globule feels the presence of the wall, we can tentatively assume for the free energy of each globule the same form in Eq. (1) with possibly modified values of the various parameters. We should consider $F(l_1, n_{c1}) + F(N - l_1, n_{c2})$. Since we do not know σ, α, and C, we first try to fit our data for $F(l_1, n_{c1}) + F(N - l_1, n_{c2}) - [F(l_1, n_{c2}) + F(N - l_1, n_{c1})]$, which should depend only on the topological correction. As shown in Fig. 5(c) for $n_{c1} = 3$, $n_{c2} = 4$, there is a remarkable agreement of our data in the whole range of N and l_1 values explored, if one puts $C \simeq 86$, while keeping $a \simeq 1.45$. This large value of C is about half the estimated one in absence of wall [10]. Thus, our free energy ansatz could account more completely for our data. In plotting $F(l_1, n_{c1}) + F(N - l_1, n_{c2})$ we are helped by the circumstance that the term $\propto \log N$ plays an almost irrelevant role in comparison with the other ones (below we use $\alpha = 1/2$). Thus, by keeping $C \simeq 86$, we can fix σ by matching our data for $P(l_1/N) \propto \exp\{[F(l_1, 3) + F(N - l_1, 4)]/k_B T\}$ [Fig. 5(d)]. The agreement is quite satisfactory if one puts $\sigma \simeq -0.98$. The ratio between the P computed at the stable maximum and that at the unstable one is almost independent of N. The same values of C and σ produce satisfactory agreement also for the plots of $P(l_1/N)$ in Fig. 5(a) for the case $3_1\#3_1$ vs 6_1. In all cases, for N sufficiently large, stable and unstable minima of the free energy occur when one of the loops has length close to the minimal one allowed by the given hosted knot in the cubic lattice [19].

Thus, a topological mechanism explains why the stable configuration is that in which the globule with smaller n_c is reduced to a minimal size while the other takes most of the ring length. This novel phenomenon should be relevant, e.g., for a slow dynamics of translocation of globular knotted ring polymers through membrane pores.

Putting things in perspective, although necessarily limited to the less complex knots, our results are accurate enough to clearly qualify n_c as the invariant controlling delocalization in the globular phase and determine unexpected thermodynamic effects of genuinely topological nature. The outlined scenario is totally different from that expected in the swollen polymer regime [3,8,20]. Even if unusually long rings need to be considered in order to fully clarify their asymptotics, the discovered phenomena are most relevant in practice for finite N.

This work is supported by "Fondazione Cassa di Risparmio di Padova e Rovigo" within the "Progetti di Eccellenza" program.

[1] E. Orlandini and S. G. Whittington, Rev. Mod. Phys. **79**, 611 (2007).
[2] C. C. Adams, *The Knot Book* (Freeman, New York, 1994).
[3] B. Marcone, E. Orlandini, A. L. Stella, and F. Zonta, J. Phys. A **38**, L15 (2005).
[4] O. Farago, Y. Kantor, and M. Kardar, Europhys. Lett. **60**, 53 (2002).
[5] M. Baiesi, E. Orlandini, and A. L. Stella, J. Stat. Mech. (2010) P06012.
[6] M. Baiesi, G. T. Barkema, and E. Carlon, Phys. Rev. E **81**, 061801 (2010).
[7] C. Vanderzande, *Lattice Models of Polymers* (Cambridge University Press, Cambridge, England, 1998).
[8] B. Marcone, E. Orlandini, A. L. Stella, and F. Zonta, Phys. Rev. E **75**, 041105 (2007).
[9] P. Virnau, Y. Kantor, and M. Kardar, J. Am. Chem. Soc. **127**, 15 102 (2005).
[10] M. Baiesi, E. Orlandini, and A. L. Stella, Phys. Rev. Lett. **99**, 058301 (2007).
[11] N. Madras and G. Slade, *The Self-Avoiding Walk* (Birkhäuser, Boston, 1993).
[12] A. L. Owczarek, T. Prellberg, and R. Brak, Phys. Rev. Lett. **70**, 951 (1993).
[13] M. C. Tesi, E. J. Janse Van Rensburg, E. Orlandini, and S. G. Whittington, J. Stat. Phys. **82**, 155 (1996).
[14] A. Y. Grosberg and A. R. Khokhlov, in *Statistical Physics of Macromolecules*, AIP Series in Polymers and Complex Materials, edited by R. Larson and P. A. Pincus (AIP, New York, 1994).
[15] J. J. Kasianowicz, E. Brandin, D. Branton, and D. W. Deamer, Proc. Natl. Acad. Sci. U.S.A. **93**, 13 770 (1996).
[16] R. M. M. Smeets, U. F. Keyser, D. Krapf, M. Y. Wu, N. H. Dekker, and C. Dekker, Nano Lett. **6**, 89 (2006).
[17] D. Marenduzzo, E. Orlandini, A. Stasiak, d. W. Sumners, L. Tubiana, and C. Micheletti, Proc. Natl. Acad. Sci. U.S.A. **106**, 22269 (2009).
[18] R. Matthews, A. A. Louis, and J. M. Yeomans, Phys. Rev. Lett. **102**, 088101 (2009).
[19] E. J. Janse van Rensburg and S. D. Promislow, J. Knot Theory Ramif. **4**, 115 (1995).
[20] R. Zandi, Y. Kantor, and M. Kardar, ARI, Bull. ITU **53**, 6 (2003).